

## **ULTIMATE BEARING CAPACITY OF STRIP FOOTING ON SAND UNDERLAIN BY CLAY UNDER INCLINED LOAD**

Rakesh Kumar DUTTA<sup>1</sup>, Vishwas Nandkishor KHATRI<sup>2</sup>, Nitesh KAUNDAL<sup>3</sup>

<sup>1</sup>Department of Civil Engineering, National Institute  
of Technology, Hamirpur, India

<sup>2</sup>Department of Civil Engineering, Indian Institute  
of Technology Dhanbad, Dhanbad, India

<sup>3</sup>PG Student, Department of Civil Engineering, National Institute  
of Technology, Hamirpur, India

### **Abstract**

This paper presents the bearing capacity determination of strip footing placed on sand underlain by clay and subjected to inclined loading. The bearing capacity equation is derived within the framework of limit equilibrium by following the projected area approach. The inclinations of load spread were selected by performing an additional finite element analysis. A parametric study was conducted to highlight the effect of various input parameters such as i) the thickness of the top sand layer, ii) embedment depth of footing, iii) the friction angle of sand and cohesion of clay, and iv) inclination of the applied load. The obtained results for a vertically loaded footing are slightly underestimated with that available in the literature. The computed bearing capacity values for a foundation with inclined loading compare favorably for lower inclination angle but slightly overestimates for higher load inclination angle, concerning that obtained using the available formula in the literature.

**Keywords:** strip footing, bearing capacity, projected area approach, layered soil, inclined loading

---

<sup>2</sup> Corresponding author: Department of Civil Engineering, Indian Institute of Technology Dhanbad, Dhanbad, Jharkhand 826004, India, e-mail: vishwas@iitism.ac.in

## 1. INTRODUCTION

The superstructure load is safely transferred to the soil through the foundation to avoid its shear failure. In this regard, the bearing capacity of a foundation is determined by assuming the soil to be homogeneous. Hence the shear strength parameters averaged up to the depth of influence of applied load are considered for the analysis. However, the soils are seldom homogeneous and instead often deposited in layers. The effect of this non-homogeneity soil and, consequently, the assumption of equivalent homogeneous material may lead to incorrect determination of bearing capacity in some instances. A typical situation implies the foundation placed on dense sand underlain by soft clay. The available solutions in the literature in this regard are primarily based on the experimental work and formulas developed thereof using the well-known limit equilibrium method<sup>[1-8]</sup>. For instance, the punching shear mechanism and limit equilibrium terminology for determining the bearing capacity of shallow foundation on layered strata comprises dense soil underlain by loose soil<sup>[8]</sup>. Following<sup>[8]</sup>, the use of the proposed theory for foundation subjected to inclined loads was extended<sup>[2]</sup>.

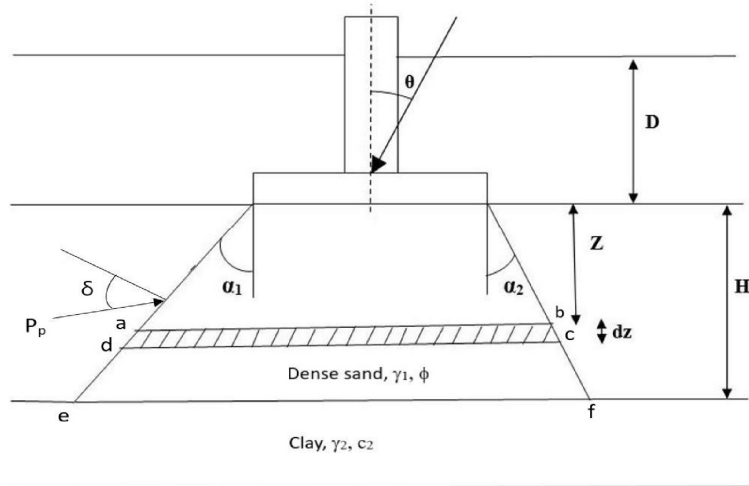
Further, design charts for bearing capacity estimation of foundation on dense sand overlying weak clay were developed<sup>[3]</sup>. Laboratory experiments were performed<sup>[7]</sup> to determine the bearing capacity of the foundation on sand underlain by clay. It was reported that a thin layer of clay below sand reduces the bearing capacity of the foundation resting on granular soil even if the clay is present at a great depth. A kinematic approach and a collapse mechanism were followed<sup>[10]</sup> to estimate the upper bound on the bearing capacity of footing on layered soil. The finite elements and finite difference approach respectively were used<sup>[9]</sup> for the analysis of the punching shear model<sup>[6]</sup> and kinematic model<sup>[10]</sup>. The study<sup>[5]</sup> suggests that the local shear failure condition and the use of Vesic and the Terzaghi's reduction factors provided better and reliable results for the case bearing capacity on the layered soil. A theory was presented<sup>[8]</sup> for the bearing capacity of footing resting over a thin sand layer lying on the clay layer extended to great depth. The centrifuge tests were performed to determine the failure mechanism. It was reported that the punching shear coefficient proposed<sup>[3]</sup> is independent of lower clay soil. A projected area approach was used<sup>[1]</sup> for load spreading together with limit equilibrium and developed a new equation for the determination of bearing capacity of footing in relation to the upper and lower layer of the soil, the footing depth to width ratio, the thickness of the top layer following similar to the approach reported in the literature<sup>[3,6]</sup>. The bearing capacity in shallow foundations was analyzed in layered strata<sup>[11]</sup> comprises of clay layer under sand by assuming the punching shear failure in the upper layer and Prandtl failure mechanism in the lower clay layer, which is weak and soft. It was attempted<sup>[12]</sup> to compare the numerical results with the plate load test data for

the bearing capacity of circular footing resting on granular soil overlying soft clay. The analytical formula was derived<sup>[4,13]</sup> to determine the bearing capacity of the strip and circular footing, respectively, by following an approach similar to the one reported in the literature<sup>[2,6]</sup>. Recently, the use of discontinuity layout optimization technique was explored<sup>[14]</sup> to determine the bearing capacity of obliquely loaded footing, which lies over dense sand over the clay layer. The accuracy of the presented data was demonstrated by validating the theory with the literature. A careful review of the literature indicates that available solutions relating to the bearing capacity assessment of shallow foundations on layered soil are subjected to vertical load. Studies on footings on layered soils are available in literature<sup>[15-25]</sup> but very limited studies for the footings on layered soil with inclined loading exists in literature<sup>[2,14]</sup>. The present study tries to address this gap. Following<sup>[4, 13]</sup>, in the present study, an analytical formula for the bearing capacity of strip footing on sand underlain by clay was derived by following punching shear mechanism and limit equilibrium methodology. The load spread mechanism in the top layer was selected by performing the finite element analysis to have a reasonable estimate of bearing capacity. The bearing capacity was determined for different values of friction angle of the top sand layer and cohesion of the bottom layer. The obtained results were compared with the literature.

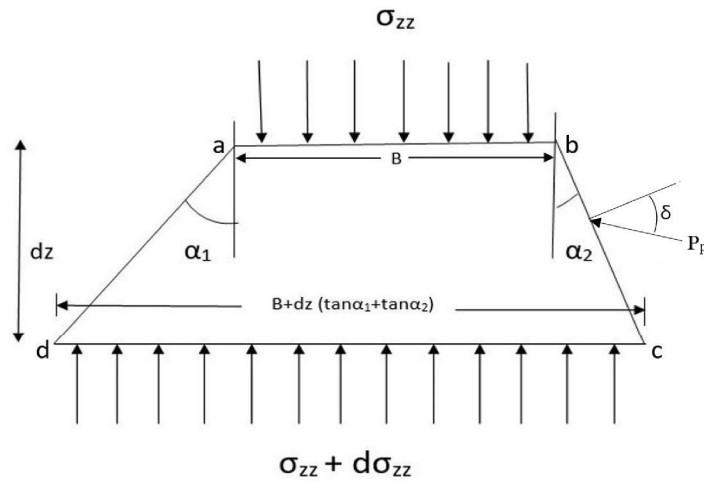
## 2. METHODOLOGY

Following the limit equilibrium-based approaches<sup>[1,3-4,6,13]</sup>, the load from the footing was assumed to spread through the top dense sand to the bottom clay soil. Accordingly, the developed failure mechanism is shown in Fig 1 (a). In this figure,  $D$ ,  $H$ ,  $B$  and  $\theta$  represents the embedment depth of footing, the thickness of the top dense sand layer, the width of footing, and the inclination of the applied load. Angle  $\alpha_1$  and  $\alpha_2$  are associated with the load spread mechanism and  $P_p$  passive pressure inclined at  $\delta$ . The bearing capacity failure was assumed to occur in the clay soil at the bottom of the projected area, far from the footing's base. Before the analysis of the problem, few assumptions are made as:

1. The sand layer is assumed in drained condition with friction angle  $\phi$ , whereas the bottom clay layer is in undrained condition with cohesion  $c_2$ .
2. The shear strength of sand and clay is fully mobilized in zones of failure.
3. The soil above the base level of the footing is taken as a surcharge having no shear strength contribution.
4. The footing is considered rigid and rough.
5. The loads considered here are inclined but concentric.
6. The passive pressure on both sides of the projected area was assumed to be equal<sup>[2]</sup>.



(a)



(b)

Fig. 1. (a) Assumed mechanism for analysis and (b) free-body diagram of strip abcd

The free-body diagram of the strip at depth  $z$  is shown in Fig 1(b). The passive earth pressure  $dP_p$  acts on the trapezoidal failure surface at an angle  $\delta$ , which is normal to the surface  $bc$  or  $ad$ . The  $\sigma_{zz}$  and  $\sigma_{zz} + d\sigma_{zz}$  are the vertical components of applied stress, on top and at the base of the section, i.e.,  $ab$  and  $dc$ , respectively. For the equilibrium of forces in a vertical direction:

$$\Sigma \mathbf{F}_v = \mathbf{0}$$

$$\sigma_{zz}(B + z \tan \alpha_1 + z \tan \alpha_2) - (\sigma_{zz} + d\sigma_{zz})[B + (z + dz) \tan \alpha_1 + (z + dz) \tan \alpha_2] - dP_{p.v}.dz + \gamma_1 dz \left( B + \frac{dz}{2} \tan \alpha_1 + \frac{dz}{2} \tan \alpha_2 + z \tan \alpha_1 + z \tan \alpha_2 \right) = 0 \quad (2.1)$$

where,  $\gamma_1$  is the unit weight of the sand layer, and  $dP_{p.v}$  is the vertical component of passive earth pressure. Note that the passive pressure on either side of the projected area is not equal; however, they were assumed the same following [2]. The  $dP_{p.v}$  is related to  $dP_p$  as:

$$dP_{p.v} = dP_{pV1} + dP_{pV2} = dP_p \sin \delta (\cos \alpha_1 + \cos \alpha_2) \quad (2.2)$$

where,

$$dP_p = K_p \gamma_1 \left[ D + z + \frac{dz}{2} \right] \quad (2.3)$$

The passive earth pressure coefficient  $K_p$  in the above expression [26] is taken using the limit equilibrium approach.

$$dP_{p.v} = K_p \gamma_1 \left[ D + z + \frac{dz}{2} \right] \sin \delta (\cos \alpha_1 + \cos \alpha_2) \quad (2.4)$$

On simplification of equation 2.1

$$-((d\sigma_{zz} B + d\sigma_{zz} z \tan \alpha_1 + d\sigma_{zz} dz \tan \alpha_1) + (d\sigma_{zz} z \tan \alpha_2 + d\sigma_{zz} dz \tan \alpha_2)) - dP_{p.v} dz + \gamma_1 dz B + \gamma_1 dz \frac{dz}{2} \tan \alpha_1 + \gamma_1 dz \frac{dz}{2} \tan \alpha_2 + \gamma_1 z dz \tan \alpha_1 + \gamma_1 z dz \tan \alpha_2 = 0 \quad (2.5)$$

Neglecting smaller terms, i.e.  $d\sigma_{zz} dz \tan \alpha_1$ ,  $d\sigma_{zz} z \tan \alpha_2$  and substituting for  $dP_{p.v}$

$$-[d\sigma_{zz}(B + (z + dz) \tan \alpha_1) + d\sigma_{zz} \tan \alpha_2 (z + dz)] - \left( \gamma_1 K_p \left( D + z + \frac{dz}{2} \right) \sin \delta (\cos \alpha_1 + \cos \alpha_2) \right) dz + \gamma_1 dz B + \gamma_1 dz \frac{dz}{2} \tan \alpha_1 + \gamma_1 dz \frac{dz}{2} \tan \alpha_2 + \gamma_1 z dz \tan \alpha_1 + \gamma_1 z dz \tan \alpha_2 = 0 \quad (2.6)$$

Neglecting the terms  $0.5\gamma_1 K_p dz \cdot dz \sin \delta (\cos \alpha_1 + \cos \alpha_2)$ ,  $0.5\gamma_1 dz \cdot dz \tan \alpha_1$ ,  $0.5\gamma_1 dz \cdot dz \tan \alpha_2$  the above equation becomes

$$-d\sigma_{zz}[B + (z + dz)(\tan \alpha_1 + \tan \alpha_2)] - \gamma_1 K_p D \sin \delta (\cos \alpha_1 + \cos \alpha_2) dz - \gamma_1 K_p z \sin \delta (\cos \alpha_1 + \cos \alpha_2) dz + \gamma_1 dz (B + z(\tan \alpha_1 + \tan \alpha_2)) = 0 \quad (2.7)$$

Rearranging the terms

$$d\sigma_{zz}[B + (z + dz)(\tan \alpha_1 + \tan \alpha_2)] = (-\gamma_1 K_p D \sin \delta (\cos \alpha_1 + \cos \alpha_2) dz - \gamma_1 K_p z \sin \delta (\cos \alpha_1 + \cos \alpha_2) dz + \gamma_1 dz (B + z(\tan \alpha_1 + \tan \alpha_2))) \quad (2.8)$$

On neglecting the term  $d\sigma_{zz} dz (\tan \alpha_1 + \tan \alpha_2)$  and rearranging we get

$$d\sigma_{zz} = \frac{-\gamma_1 K_P D \sin \delta (\cos \alpha_1 + \cos \alpha_2) dz}{[B+z(\tan \alpha_1 + \tan \alpha_2)]} - \frac{\gamma_1 K_P z \sin \delta (\cos \alpha_1 + \cos \alpha_2) dz}{[B+z(\tan \alpha_1 + \tan \alpha_2)]} + \gamma_1 dz \quad (2.9)$$

Integrating both sides in equation (2.9), we get

$$\int d\sigma_{zz} = \int \frac{-\gamma_1 K_P D \sin \delta (\cos \alpha_1 + \cos \alpha_2) dz}{[B+z(\tan \alpha_1 + \tan \alpha_2)]} - \int \frac{\gamma_1 K_P z \sin \delta (\cos \alpha_1 + \cos \alpha_2) dz}{[B+z(\tan \alpha_1 + \tan \alpha_2)]} + \int \gamma_1 dz \quad (2.10)$$

Let

$$A_1 = -\gamma_1 K_P D \sin \delta (\cos \alpha_1 + \cos \alpha_2) \quad (2.11a)$$

$$A_2 = -\gamma_1 K_P \sin \delta (\cos \alpha_1 + \cos \alpha_2) \quad (2.11b)$$

Also,

$$u = B + z(\tan \alpha_1 + \tan \alpha_2) \quad (2.12a)$$

$$du = dz(\tan \alpha_1 + \tan \alpha_2) \quad (2.12b)$$

$$dz = \frac{du}{(\tan \alpha_1 + \tan \alpha_2)}$$

The equation 2.10 can be rewritten using the transformations shown in equations 2.11 and 2.12, as:

$$\sigma_{zz} = A_1 \int \frac{1}{u(\tan \alpha_1 + \tan \alpha_2)} du + A_2 \int \frac{z}{u(\tan \alpha_1 + \tan \alpha_2)} du + \int \gamma_1 dz \quad (2.13)$$

On integrating the above equation, we get:

$$A_1 \int \frac{1}{B + z(\tan \alpha_1 + \tan \alpha_2)} dx = \frac{A_1}{(\tan \alpha_1 + \tan \alpha_2)} \ln[B + z(\tan \alpha_1 + \tan \alpha_2)] + C_1 \quad (2.14a)$$

$$A_2 \int \frac{z}{B + z(\tan \alpha_1 + \tan \alpha_2)} dz = \frac{A_2}{(\tan \alpha_1 + \tan \alpha_2)^2} [B + z(\tan \alpha_1 + \tan \alpha_2) - B \ln B + z(\tan \alpha_1 + \tan \alpha_2)] + C_2 \quad (2.14b)$$

and

$$\int \gamma_1 dz = \gamma_1 z + C_3 \quad (2.14c)$$

Hence, combining equations 2.14(a)-2.14(c), we get:

$$\sigma_{zz} = \frac{A_1}{(\tan \alpha_1 + \tan \alpha_2)} \ln[B + z(\tan \alpha_1 + \tan \alpha_2)] + \frac{A_2}{(\tan \alpha_1 + \tan \alpha_2)^2} [B + z(\tan \alpha_1 + \tan \alpha_2) - B \ln B + z(\tan \alpha_1 + \tan \alpha_2)] + \gamma_1 z + C \quad (2.15)$$

Now, substituting values of A1 and A2 from equation (2.11), the above equation becomes:

$$\sigma_{zz} = \frac{-\gamma_1 K_P D \sin \delta (\cos \alpha_1 + \cos \alpha_2)}{(\tan \alpha_1 + \tan \alpha_2)} \ln[B + z(\tan \alpha_1 + \tan \alpha_2)] - \frac{\gamma_1 K_P \sin \delta (\cos \alpha_1 + \cos \alpha_2)}{(\tan \alpha_1 + \tan \alpha_2)^2} [B + z(\tan \alpha_1 + \tan \alpha_2) - B \ln B + z(\tan \alpha_1 + \tan \alpha_2)] + \gamma_1 z + C \quad (2.16)$$

The boundary condition is applied to find the integration constant C, as per the following:

$$\text{At } z = 0 \quad \sigma_{zz} = q_u \quad (2.17)$$

Where  $q_u$  is the ultimate bearing capacity of the footing.

$$q_u = \frac{-\gamma_1 K_P D \sin \delta (\cos \alpha_1 + \cos \alpha_2)}{(\tan \alpha_1 + \tan \alpha_2)} \ln[B] - \frac{\gamma_1 K_P \sin \delta (\cos \alpha_1 + \cos \alpha_2)}{(\tan \alpha_1 + \tan \alpha_2)^2} [B - B \ln[B]] + C \quad (2.18)$$

Therefore,

$$C = q_u + \frac{\gamma_1 K_P \sin \delta (\cos \alpha_1 + \cos \alpha_2)}{(\tan \alpha_1 + \tan \alpha_2)} [D \ln(B) + \frac{B(1-\ln(B))}{(\tan \alpha_1 + \tan \alpha_2)}] \quad (2.19)$$

Now, at  $z = H$ ,  $\sigma_{zz} = q_b$

Where  $q_b$  = bearing capacity of the bottom layer below.

Therefore

$$\sigma_{zz} = q_b = \frac{-\gamma_1 K_P D \sin \delta (\cos \alpha_1 + \cos \alpha_2)}{(\tan \alpha_1 + \tan \alpha_2)} [\ln(B + H(\tan \alpha_1 + \tan \alpha_2))] - \frac{\gamma_1 K_P \sin \delta (\cos \alpha_1 + \cos \alpha_2)}{(\tan \alpha_1 + \tan \alpha_2)^2} [(B + H(\tan \alpha_1 + \tan \alpha_2)) - B \ln(B + H(\tan \alpha_1 + \tan \alpha_2))] + \gamma_1 H + q_u + \frac{\gamma_1 K_P \sin \delta (\cos \alpha_1 + \cos \alpha_2)}{(\tan \alpha_1 + \tan \alpha_2)} [D \ln(B) + \frac{B(1-\ln(B))}{(\tan \alpha_1 + \tan \alpha_2)}] \quad (2.20)$$

On simplification, the above expression becomes

$$q_u = q_b + \frac{\gamma_1 K_P D \sin \delta (\cos \alpha_1 + \cos \alpha_2)}{(\tan \alpha_1 + \tan \alpha_2)} [\ln(B + H(\tan \alpha_1 + \tan \alpha_2)) - \ln(B)] + \frac{\gamma_1 K_P \sin \delta (\cos \alpha_1 + \cos \alpha_2)}{(\tan \alpha_1 + \tan \alpha_2)^2} [H(\tan \alpha_1 + \tan \alpha_2) - B(\ln(B + H(\tan \alpha_1 + \tan \alpha_2)) - \ln(B))] - \gamma_1 H \quad (2.21)$$

Now let,  $F = \ln(B + H(\tan \alpha_1 + \tan \alpha_2)) - \ln(B) = \ln \frac{(B + H(\tan \alpha_1 + \tan \alpha_2))}{B}$

Therefore

$$q_u = q_b + \frac{\gamma_1 K_P D \sin(\cos\alpha_1 + \cos\alpha_2)}{(\tan\alpha_1 + \tan\alpha_2)} [F] + \frac{\gamma_1 K_P \sin\delta(\cos\alpha_1 + \cos\alpha_2)}{(\tan\alpha_1 + \tan\alpha_2)^2} [H(\tan\alpha_1 + \tan\alpha_2) - \text{B.F.}] - \gamma_1 H \quad q_u = q_b + \frac{\gamma_1 K_P \sin\delta(\cos\alpha_1 + \cos\alpha_2)}{(\tan\alpha_1 + \tan\alpha_2)} \left[ DF + H - \frac{\text{B.F.}}{(\tan\alpha_1 + \tan\alpha_2)} \right] - \gamma_1 H \quad (2.22)$$

Converting the above equation in dimensionless form by dividing with  $\gamma_1 B$  and further simplifying we get

$$\frac{q_u}{\gamma_1 B} = \frac{q_b}{\gamma_1 B} - \frac{H}{B} + \frac{K_P \sin\delta(\cos\alpha_1 + \cos\alpha_2)}{(\tan\alpha_1 + \tan\alpha_2)} \left[ \frac{\text{D.F.}}{B} + \frac{H}{B} - \frac{F}{(\tan\alpha_1 + \tan\alpha_2)} \right] \quad (2.23)$$

The above expression of bearing capacity determination of strip footing on dense soil underlain by loose soil is very general. For the present situation of sand underlain by clay, the bearing capacity of the second layer is prescribed as:

$$q_b = c_2 N_{c2} i_{c2} + \gamma_1 (H + D) i_{q2} \quad (2.24)$$

Where,  $c_2$  = cohesion,  $N_{c2}$  = bearing capacity factor  $N_c$  for clay and  $i_{c2}$  and  $i_{q2}$  = inclination factors.

As indicated by equation (2.23), the bearing capacity of strip footing on layered soil and subjected to inclined loading depends on (i) embedment depth of footing (D), (ii) thickness of the dense sand layer (H), (iii) shear strength and unit weight of the top and bottom layer ( $\gamma_1, \phi, c_2, \gamma_2$ ), (iv) width of footing (B) and (v) inclination of load with respect to vertical ( $\theta$ ). It is pertinent to mention that the angle  $\alpha_1$  and  $\alpha_2$  associated with the load spread mechanism also depends on the above-mentioned parameters. The angles  $\alpha_1$  and  $\alpha_2$  both were taken equal to the inclination of the applied load in literature [2]. In the present study, to have a reasonable estimate of bearing capacity using the limit equilibrium methodology, the magnitude of  $\alpha_1$  and  $\alpha_2$  is determined by performing a finite element analysis in the ABAQUS software. For this study, the dense sand with friction angle ( $\phi$ )=45°, dilation angle ( $\psi$ )=12°, dry unit weight ( $\gamma_d$ ) = 22kN/m<sup>3</sup>, modulus of elasticity (E) =50 MPa and Poisson's ratio, ( $\nu$ )= 0.29 was considered. The clay was considered undrained, with cohesion ( $c_2$ ) = 21 kPa,  $\gamma$ =20 kN/m<sup>3</sup>, E=4 MPa and Poisson's ratio ( $\nu$ ) = 0.5 [12]. Both the soils were assumed to obey Mohr-Coulomb's yield criteria. The analysis was performed for plane strain conditions using four noded bilinear quadrilateral elements with hourglass control and a reduced integration scheme. The domain boundaries were so selected to contain the failure zone completely within them. Accordingly, the horizontal and vertical boundaries of 10 times footing width were finalized. The far-off vertical boundaries were allowed to deform only vertically while the bottom boundary was fixed and not allowed to move in either lateral or vertical direction. The parametric study was performed by varying the thickness ratio (H/B) and load inclination ( $\theta$ ). The footing was placed on the surface (D=0) and considered. After performing the analysis, failure patterns in various cases were generated. The variation of failure pattern with load inclination ( $\theta$ ) is depicted in Fig 2. With the study of failure patterns, the inclinations  $\alpha_1$  and  $\alpha_2$  associated with the load spread



mechanism were determined as per Fig 3. The variation of  $\alpha_1$  and  $\alpha_2$  in various cases is generated and shown in Table 1.

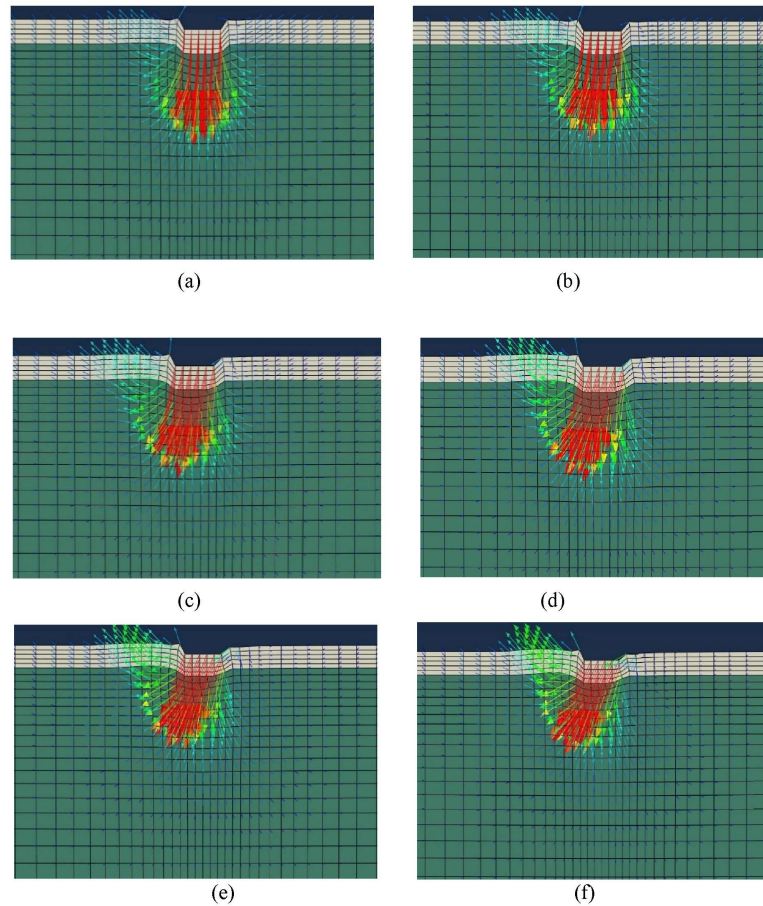


Fig. 2. Failure pattern with (a)  $\theta = 5^\circ$ , (b)  $\theta = 10^\circ$ , (c)  $\theta = 15^\circ$ , (d)  $\theta = 20^\circ$ , (e)  $\theta = 25^\circ$  (f)  $\theta = 30^\circ$

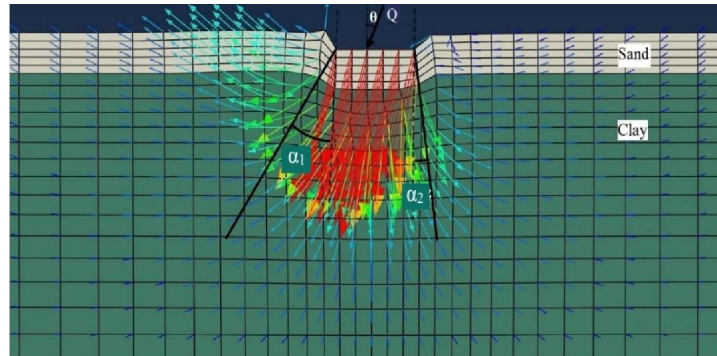


Fig. 3. Determination of angles  $\alpha_1$  and  $\alpha_2$  using failure patterns

Table 1. Variation of spread angles ( $\alpha_1, \alpha_2$ ) with load inclination ( $\theta$ ) and thickness ratio (H/B)

H/B	$\theta$	$\alpha_1$	$\alpha_2$
0.5	0	30	30
0.5	5	37	20
0.5	10	41	16
0.5	15	44	10
0.5	20	48.5	3.5
0.5	25	55	-5.5
0.5	30	63	-11.5
1	0	18.5	18.5
1	5	26.5	11
1	10	35	9
1	15	42.5	6.5
1	20	44.5	-1.5
1	25	52	-8
1	30	57.5	-10.5
1.5	0	17	17
1.5	5	20	9
1.5	10	21.5	6
1.5	15	32	1
1.5	20	34	-6
1.5	25	35	-11
1.5	30	38	-14
2	0	17	17
2	5	21	8
2	10	27	4.5
2	15	27	3
2	20	28.5	1
2	25	29.5	-2
2	30	31	-5

A curve fitting to the values shown in this table provided the equation for the determination of  $\alpha_1$  and  $\alpha_2$  as:

$$\alpha_1 = 39.304 + 0.868 \theta - 14.043 \frac{H}{B} \quad (2.25a)$$

$$\alpha_2 = 23.768 - 0.996 \theta - 3.743 \frac{H}{B} \quad (2.25b)$$

A careful study of equation 2.25 suggests that the load spread angles  $\alpha_1$  and  $\alpha_2$  is different from the load inclination ( $\theta$ ) as assumed in literature<sup>[2]</sup>. Note that the above equation is valid for the selected range of parameters for finite element analysis. One may use the developed bearing capacity equation (2.23) with the appropriate substitution of angles  $\alpha_1$  and  $\alpha_2$ ; however, in the present study, the equation (2.25) is used for the same.

### 3. VALIDATION WITH FEM RESULTS

The present bearing capacity determination using equations (23)-(25) is based on the  $\alpha_1$  and  $\alpha_2$  obtained using a finite element analysis. Hence, it was thought of validating the present bearing capacity with the F.E.M. predictions. Note that the F.E.M. analysis was performed with ( $\phi$ ) = 45°, and ( $\psi$ ) = 12°, i.e., the assumption of non-associated flow rule in the sand. However further study can be conducted by adopting non-coaxial flow rule which the beyond the scope of the present work. To account for the effect of dilatancy in the present analysis, an equivalent friction angle ( $\phi_{eq}$ ) was obtained by following the approximation reported in the literature<sup>[27]</sup> as:

$$\tan \phi_{eq} = \eta \tan \phi \quad (3.1)$$

$$\eta = \frac{\cos \psi \csc \phi}{1 - \sin \psi \sin \phi} \quad (3.2)$$

The equivalent friction angle using the above equation was determined as 39.04°. The same was used in the equations (2.23)-(2.25) for bearing capacity determination. In the bearing capacity determination of the bottom clay layer (equation 2.24), the inclination factors  $i_{c2}$  and  $i_{q2}$  were obtained by following the literature<sup>[2]</sup>. Further, the ultimate bearing capacity using F.E.M. was determined using the pressure-settlement curves by following the hyperbolic method<sup>[28]</sup>. On this basis, the comparison of present normalized bearing capacity obtained using equations (2.23)-(2.25) and finite element method is shown in Table 2. A study of this table suggests that present results compare closely with F.E.M. results for  $\theta = 0^\circ$  with a maximum deviation of 9.81 % for  $H/B = 1$ . With the increase in  $\theta$ , the current bearing capacity with the usage of equations (2.23)-(2.25) is somewhat underestimated concerning F.E.M. results. It could be due to the use of the same passive earth pressure coefficient corresponding to a vertical wall on both the edges (line ad and bc) of the projected area.

Table 2. Comparison of present analysis with the finite element method

H/B	Normalized bearing capacity ( $q_{ult}/\gamma_1 B$ )					
	$\theta = 0^\circ$		$\theta = 10^\circ$		$\theta = 20^\circ$	
	Present Equation	Present F.E.M. Analysis	Present Equation	Present F.E.M. Analysis	Present Equation	Present F.E.M. Analysis
0.5	7.06	6.64	5.54	6.14	4.14	5.90
1	12.10	13.32	10.31	11.82	8.46	10.68
1.5	20.36	22.73	18.45	21.82	16.13	20.90
2	32.84	33.64	31.13	32.32	28.49	30.90

#### 4. RESULTS AND DISCUSSIONS

With the use of equations (2.23)-(2.25), the bearing capacity of strip footing on layered soil was generated for the variation of parameters like thickness ratio (H/B), depth ratio (D/B), normalized cohesive strength for clay ( $c_2/\gamma_1 B$ ) and inclination of load ( $\theta$ ). Further, the bearing capacity was expressed in normalized form as ( $q_u/\gamma_1 B$ ). The results of this parametric study and comparison with literature are described in the subsequent sections.

##### 4.1 Variation of bearing capacity with cohesion ( $c_2$ ), friction angle ( $\phi$ ) and load inclination ( $\theta$ )

The variation of bearing capacity with the cohesion of the bottom layer ( $c_2$ ), the friction angle top sand layer ( $\phi$ ) and inclination of the load ( $\theta$ ) was generated using equation (2.23). The computations were performed for  $\phi = 30^\circ-45^\circ$ ,  $c_2/\gamma_1 B = 0.5-2$ , and  $\theta = 10^\circ-30^\circ$ . The obtained variation of bearing capacity is shown in Fig 4 and Fig. 5. From these figures, it can be noticed that for a given  $\phi$  and  $\theta$  the bearing capacity varies linearly with an increase in the normalized cohesion ( $c_2/\gamma_1 B$ ). As anticipated, for a constant friction angle ( $\phi$ ) and  $c_2/\gamma_1 B$ , the bearing capacity reduces with an increase in the obliquity of loading  $\theta$ . For instance, the normalized bearing capacity for  $c_2/\gamma_1 B = 1$ ,  $H/B = 0.5$  and  $\phi = 45^\circ$ ,  $\delta = \phi$  was estimated as 8.17 for  $\theta = 10^\circ$  which reduces to 4.99 for  $\theta = 30^\circ$ . A similar variation was observed for other cases as well.

##### 4.2 Variation of bearing capacity with thickness ratio (H/B), depth ratio (D/B)

The variation of normalized bearing capacity ( $q_u/\gamma_1 B$ ) with thickness ratio (H/B) and depth ratio (D/B) for  $c_2/\gamma_1 B = 0.5$  is shown in Fig 6 and Fig. 7, respectively. The bearing capacity was found to increase in a non-linear manner with the increase in the thickness of the top dense sand layer. Whereas for given  $c_2/\gamma_1 B$ ,

$H/B$ ,  $\phi$  and  $\theta$  of the bearing capacity increases linearly with an increase in depth ratio ( $D/B$ ).

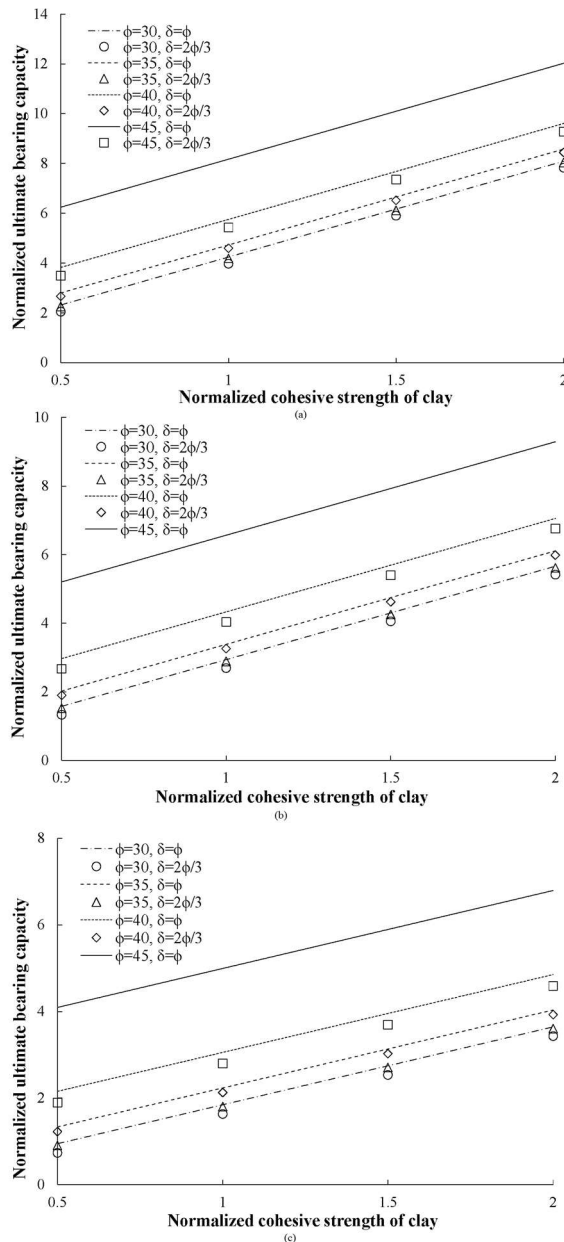


Fig. 4. Variation of normalized bearing capacity with cohesion parameter for (a)  $\theta = 10^\circ$ , (b)  $\theta = 20^\circ$  and (c)  $\theta = 30^\circ$ , at  $H/B = 0.5$ ,  $D/B = 0$

It implies that the bearing capacity of the surface or embedded footing on soft clay can be increased by adding a dense sand layer on the top of the clay layer. For instance, the normalized bearing capacity of surface footing on soft clay for  $\theta = 10^\circ$  and  $c_2/\gamma_1B = 0.5$  can be computed as 1.93 and on the addition of a dense sand layer ( $\phi = 45^\circ$ ) up to  $H/B = 2$ , the normalized bearing capacity increases to 68.87. The increase in bearing capacity seen in this case is 35.68 times the footing resting on soft clay.

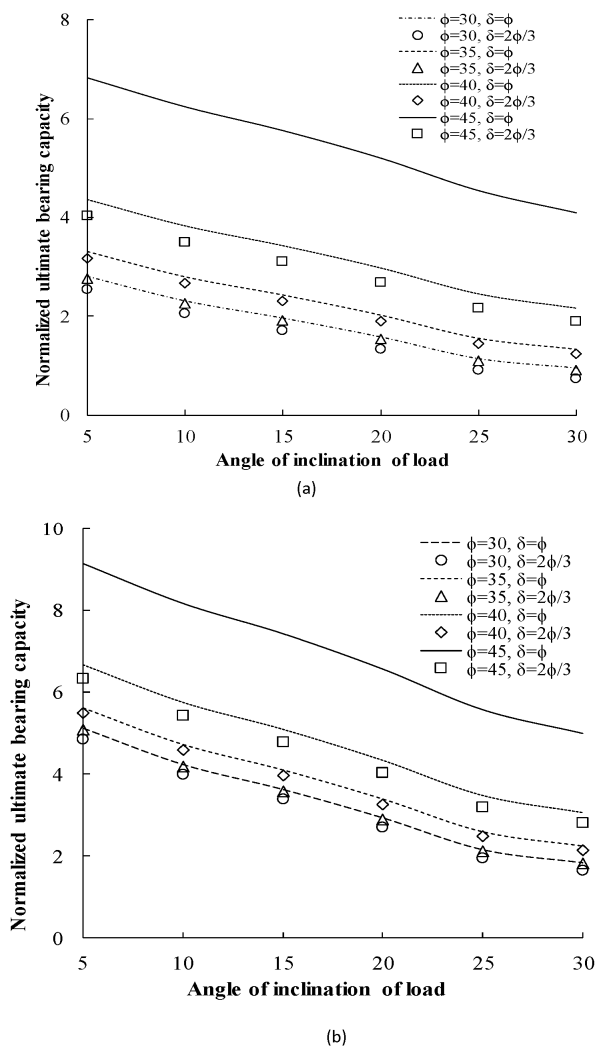
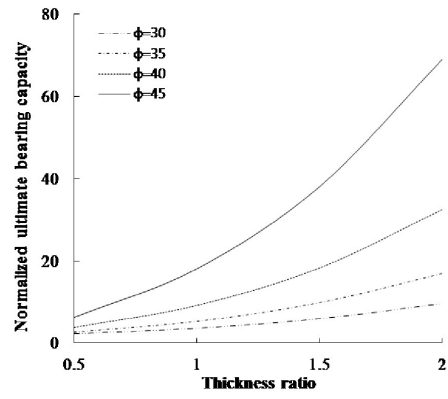
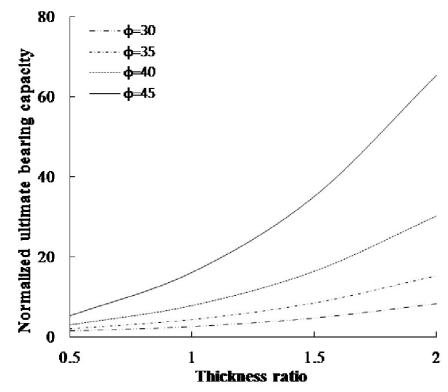


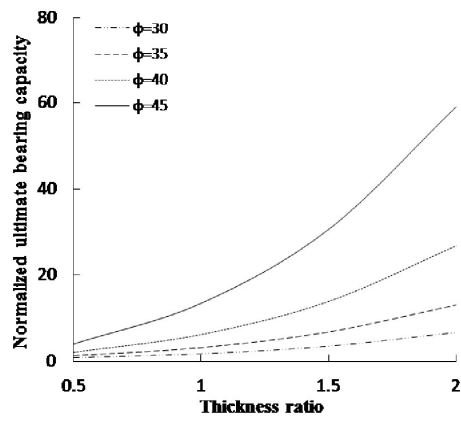
Fig. 5. Variation of normalized bearing capacity with angle of inclination of load for (a)  $c_2/\gamma_1B = 0.5$  (b)  $c_2/\gamma_1B = 1$ , at  $H/B=0.5$ ,  $D/B = 0$



(a)



(b)



(c)

Fig. 6. Variation of normalized bearing capacity with thickness ratio for (a)  $\theta = 10^\circ$ , (b)  $\theta = 20^\circ$  and (c)  $\theta = 30^\circ$ , at  $c_2/\gamma_1 B = 0.5$

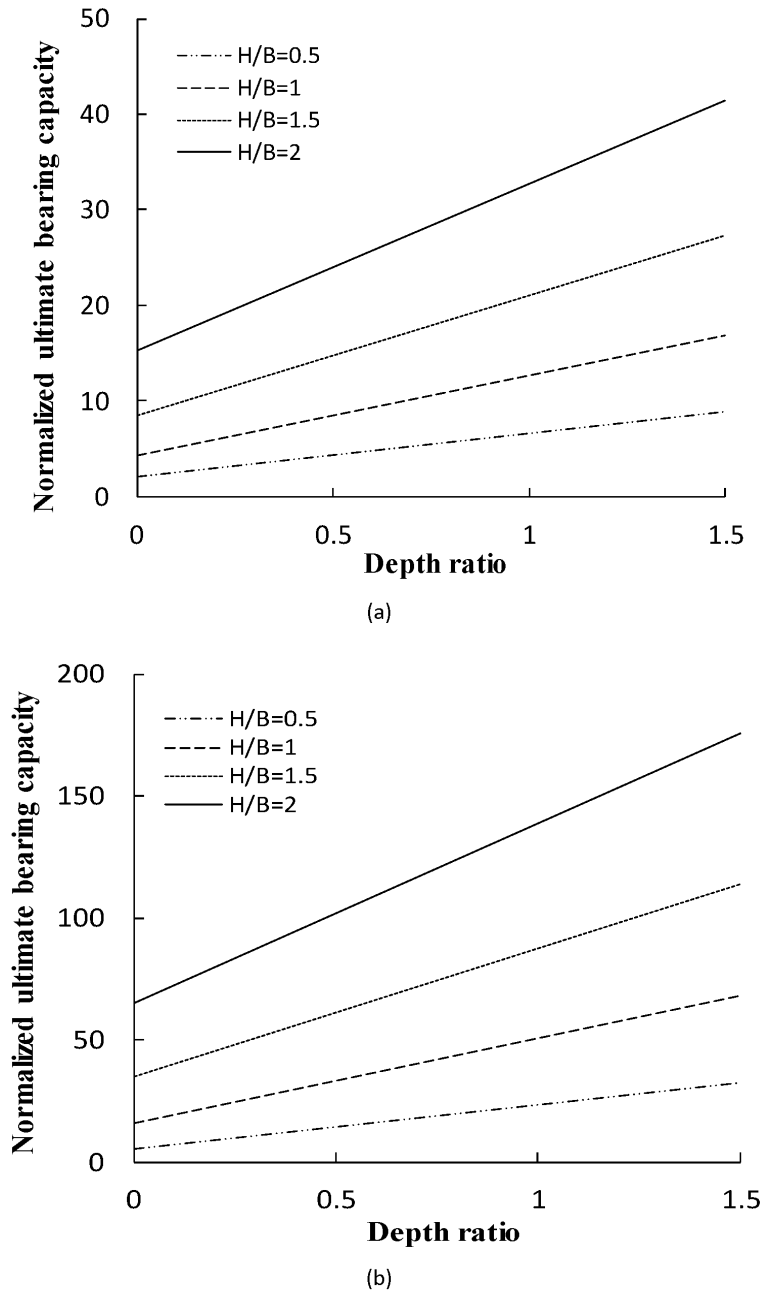
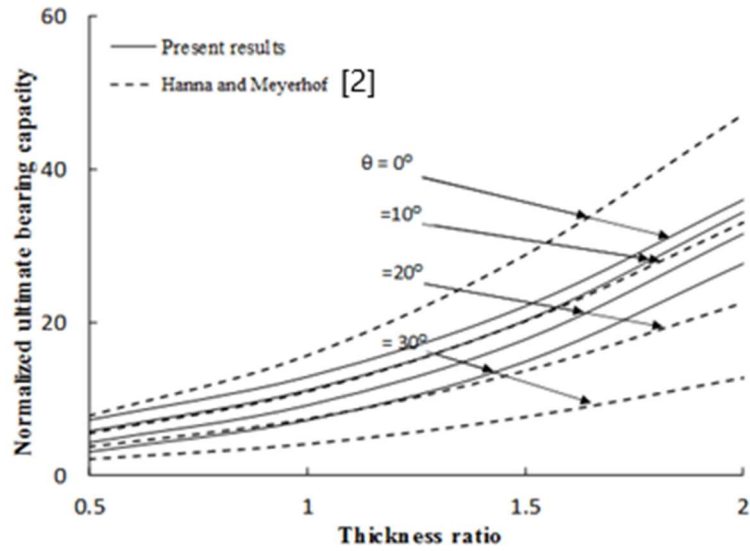


Fig. 7. Variation of normalized bearing capacity with depth ratio for (a)  $\phi = 35^\circ$  and (b)  $\phi = 45^\circ$ , at  $\theta=20^\circ$ ,  $c_2/\gamma_1B = 0.5$

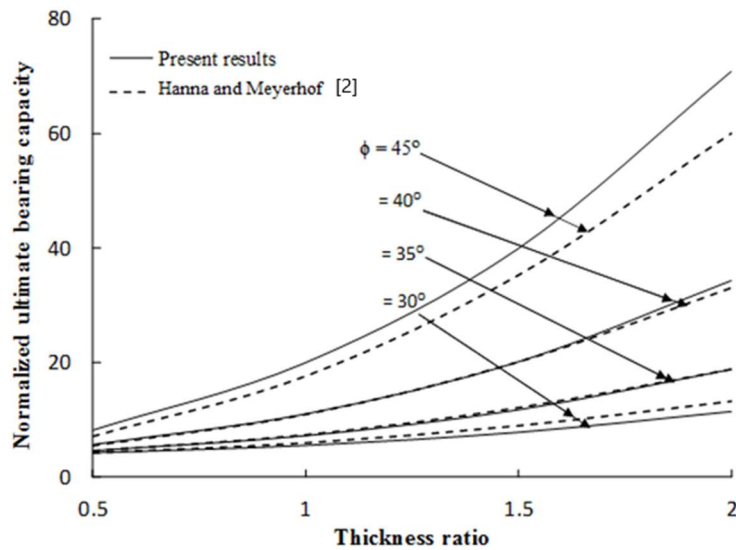


### 4.3 Comparison

As mentioned previously, the solution for footing on layered soil and subjected to inclined loading was perhaps first provided in the literature [2].



(a) Comparison at  $\phi=40^\circ$ , at  $c_2/\gamma_1 B=1$ ,  $D/B=0$



(b) Comparison at  $\theta=10^\circ$ , at  $c_2/\gamma_1 B=1$ ,  $D/B=0$

Fig. 8. Comparison of present results with literature [2] for  $c_2/\gamma_1 B=1$ ,  $D/B=0$  (a)  $\phi=40^\circ$  (b)  $\theta=10^\circ$

Hence it was thought of comparing the present results with the same. In this regard the computations were performed for  $\theta = 0^\circ\text{-}30^\circ$ ,  $\phi = 30^\circ\text{-}45^\circ$ ,  $H/B = 0.5\text{-}2$  and with  $c_2/(\gamma_1 B) = 1$  and  $D/B = 0$ . Additionally, the comparison for  $\theta = 0^\circ$ ,  $\phi = 40^\circ$ ,  $H/B = 1$  is also made with i) the upper bound solution [10], ii) numerical limit analysis solution [29] iii) discontinuity layout optimization [14] apart from the literature [2]. The relevant comparison is depicted in Fig. 8 and Fig. 9, respectively. The study of Fig. 8 suggests that the present bearing capacity values are close to the solution [2] for vertically loaded footing. The comparison shown in Fig. 9 further reaffirms that the present results for vertically loaded footing agree with that reported in the literature. It implies that the assumed load spread ( $\alpha_1$  and  $\alpha_2$ ) angles and the passive pressure coefficients are quite reasonable. In the case of footing with inclined loading, the present bearing capacity values are slightly overestimated in most of the cases except for  $\theta = 10^\circ$ ,  $20^\circ$  at  $\phi = 30^\circ$ . The difference in the present and the one reported in the literature [2] bearing capacity values is perhaps due to the use of i)  $\alpha_1 = \alpha_2 = \theta$  in the literature [2] and ii) punching shear coefficient. Note that in the present study, the magnitudes of  $\alpha_1$  and  $\alpha_2$  were selected based on finite element analysis. Further, a passive earth pressure coefficient for a vertical wall was considered instead of using the punching shear coefficient.

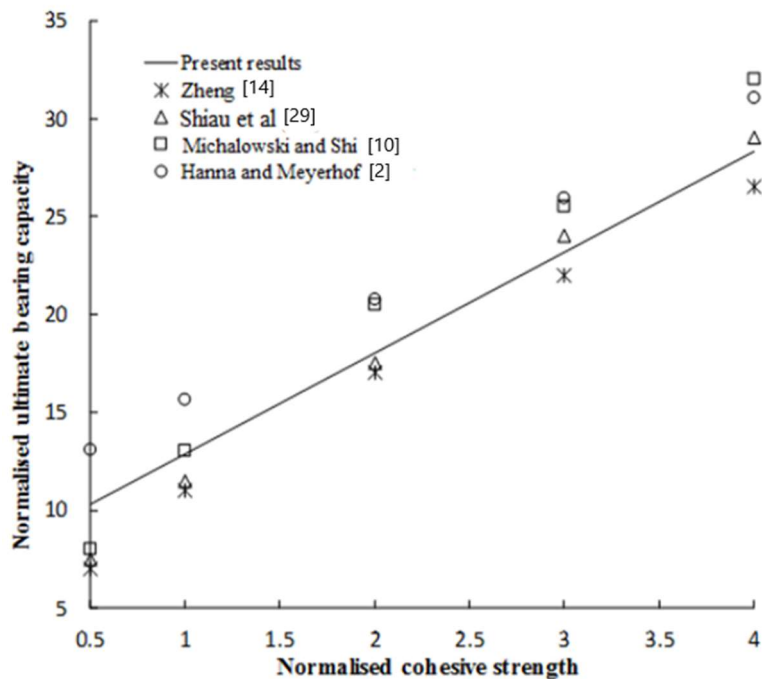


Fig. 9. Comparison of present results with literature for  $\phi = 40^\circ$ ,  $H/B = 1$  and  $\theta = 0^\circ$

## 5. CONCLUSIONS

This present work generated the bearing capacity equation for an obliquely loaded strip footing on layered soil with a sand layer on top of a clay layer by utilizing the well-known limit equilibrium approach and the load spread mechanism. The results obtained from this study bring forth the following conclusions:

1. The bearing capacity of strip footing was found to increase with an increase in i) thickness of the top sand layer, ii) friction angle of sand, iii) depth of foundation, and iii) normalized cohesion.
2. In various cases, the bearing capacity was found to decrease with an increase in the obliquity of loading. The reduction in bearing capacity with an increase  $\theta$  from  $0^\circ$  to  $30^\circ$  was up to 60 %.
3. The present finite element results were comparable with that obtained using the derived equation in many cases for a selected range of input parameters.
4. The derived bearing capacity equation was in tune with the literature for a vertically loaded footing. However, some scatter was observed for the obliquely loaded footing, which can be attributed to the difference of assumptions followed in the present and the reported studies.

## NOTATIONS

$\theta$	Angle of inclination of load, in degree
$\alpha_1, \alpha_2$	Angles of load spread in soil, in degree
$\phi$	Soil frictional angle, degree
$\delta$	Mobilised shearing resistance angle, degree
$Q$	Applied inclined load
$\sigma$	Applied stress, $\text{kN/m}^2$
$d\sigma$	Increment in stress applied, $\text{kN/m}^2$
$\sigma_{zz}$	Vertical component of applied stress, $\text{kN/m}^2$
$d\sigma_{zz}$	Vertical stress increment component, $\text{kN/m}^2$
$E$	Elastic modulus
$\nu$	Poisson ratio
$K_p$	Passive earth pressure coefficient
$\gamma_1, \gamma_2$	Unit weight of sand and clay respectively
$Z$	Depth of soil section for analysis below footing
$H$	Thickness of upper sand layer below footing
$B$	Width of footing
$D$	Depth of footing
$N_{c1}, N_{q1}, N_{\gamma1}$	Bearing capacity factors corresponds to upper sand layer
$N_{c2}, N_{q2}, N_{\gamma2}$	Bearing capacity factor corresponds to clay layer below
$c_2$	Cohesion of clay layer

OCR	Overly consolidated clay
$P_p$	Total passive earth pressure
$dP_p$	Passive earth pressure that acts section of depth $dz$
$dP_{pv}$	Vertical element of passive earth pressure that acts on section of depth $dz$
$c_2/\gamma_1 B$	Normalized cohesive strength parameter of clay
$q_u/\gamma_1 B$	Normalized ultimate bearing capacity of footing
$i_{q2}, i_{c2}$	Inclination factors [9]
$H/B$	Thickness ratio
$D/B$	Depth ratio
$C$	Integration constant

## REFERENCES

1. Farah, CA 2004. Ultimate bearing capacity of shallow foundations on layered soils. MSc Thesis, Civil and Environmental Engineering, Quebec: Concordia.
2. Hanna, AM and Meyerhof, GG 1978. Ultimate bearing capacity of foundations on layered soils under inclined load. *Can Geotech J* **15**, 565-572.
3. Hanna, AM and Meyerhof, GG 1980. Design charts for ultimate bearing capacity of foundations on sand overlying soft clay. *Can Geotech J* **17**, 300–303.
4. Joshi, VC, Dutta, RK and Shrivastava, R 2015. Ultimate bearing capacity of circular footing on layered soil. *J Geo-Eng* **10**, 25-34.
5. Kenny, MJ and Andrawes, KZ 1997. The bearing capacity of footings on sand layer overlying soft clay. *Geotechnique* **47**, 339–345.
6. Meyerhof, GG 1974. Ultimate bearing capacity of footings on sand layer overlying clay. *Can Geotech J* **11**, 223–229.
7. Oda, M and Win, S 1990. Ultimate bearing capacity tests on sand with clay layer. *J Geotech Eng* **116**, 1902–1906.
8. Okamura, M, Takemura, J and Kimura, T 1998. Bearing capacity predictions of sand overlying clay based on limit equilibrium methods. *Soils Found* **38**, 181–194.
9. Burd, HJ and Frydman, S 1997. Bearing capacity of plane-strain footing on layered soils. *Can Geotech J* **34**, 241–253.
10. Michalowski, RL and Shi, L 1995. Bearing capacity of footings over two-layer foundations soil. *J Geotech Eng* **121**, 421–428.
11. Abdulhaz, O, Al-Shenawy, A, Awad, A and Al-Karni, A 2005. Derivation of bearing capacity equation for a two layered system of weak clay layer overlaid by dense sand layer. *Pertan J Sci Technol* **13**, 213–235.
12. Ismail Ibrahim, KMH 2016. Bearing capacity of circular footing resting on granular soil overlying soft clay. *HBRC Journal*. **12(1)**, 71-77.

13. Gupta A, Dutta, RK, Shrivastava, R and Khatri, VN 2017. Ultimate bearing capacity of Square/Rectangular footing on layered soil. *Indian Geotech J.* **47**, 303–313.
14. Zheng, G, Zhao, J, Zhou, H and Zhang, T 2019. Ultimate bearing capacity of strip footings on sand overlying clay under inclined loading. *Computers and Geotechnics* **106**, 266-273.
15. Hanna, AM and Meyerhof, G 1979. Ultimate bearing capacity of foundations on a three-layer soil, with special reference to layered sand. *Canadian Geotechnical Journal* **16(2)**, 412– 414.
16. Pfeifle, TW and Das, BM. Model Tests for Bearing capacity of in Sand. *Journal of Geotechnical Engineering*, ASCE, 105(GT9), 1112-1116.
17. Hanna, AM 1981. Experimental Study of Footings in Layered Soil. *Journal of Geotechnical Engineering*, ASCE, vol. 107, no.GT8, 1113-1127.
18. Hanna, AM 1982. Bearing capacity of foundations on a weak sand layer overlying a strong deposit. *Canadian Geotechnical Journal* **19(3)**, 392–396. <http://dx.doi.org/10.1139/t82-043>
19. Georgiadis, M and Michalopoulos, A 1985. Bearing capacity of gravity bases on layered soil. *Journal of Geotechnical Engineering ASCE* **111(6)**, 712–729. [http://dx.doi.org/10.1061/\(ASCE\)0733-9410\(1985\)111:6\(712\)](http://dx.doi.org/10.1061/(ASCE)0733-9410(1985)111:6(712))
20. Hanna, AM 1987. Finite element analysis of footings on layered soils. *Mathematical Modelling* **9(11)**, 813–819. [http://dx.doi.org/10.1016/0270-0255\(87\)90501-X](http://dx.doi.org/10.1016/0270-0255(87)90501-X)
21. Madhav, MR and Sharma, JSN 1991. Bearing capacity of clay overlain by stiff soil. *Journal Geotechnical Engineering* **117(12)**, 1941–1947.
22. Merifield, RS, Sloan, SW and Yu, HS 1999. Rigorous solutions for the bearing capacity of two layered clay soils. *Géotechnique* **49(4)**, 471–490.
23. Abdulhahz, O, Al-Shenawy, A, Awad, A and Al-Karni, A. 2005. Derivation of bearing capacity equation for a two layered system of weak clay layer overlaid by dense sand layer. *Pertanika Journal of Science & Technology* **13(2)**, 213–235.
24. Loukidis, D, Chakraborty, T and Salgado, R. 2008. Bearing capacity of strip footings on purely frictional soil under eccentric and inclined loads. *Canadian Geotechnical Journal* **4**, NRC Canada. <http://doi:10.1139/T08-015>
25. Mosadegh, A and Nikraz, H 2015. Bearing capacity of footing on a layered soil using ABAQUS. *Journal of Earth Science and Climate Change* **6**. <http://dx.doi.org/10.4172/2157-7617.1000264>
26. Patki, MA, Mandal, JN and Dewaikar, DM 2015. Computation of passive earth pressure coefficients for a vertical retaining wall with inclined cohesionless backfill. *Int J Geo-Eng* **6**, 4.

27. Drescher, A and Detournay, E 1993. Limit load in translational failure mechanisms for associative and non-associative materials. *Geotechnique* **43**, 443-456.
28. Kondner, RL 1963. Hyperbolic stress-strain response: cohesive soils. *J Soil Mech Found Eng.* **89**,115-141.
29. Shiau, JS, Lyamin, AV and Sloan, SW 2003. Bearing capacity of sand layer on clay by finite element limit analysis. *Can Geotech J* **40**, 900-915.

*Editor received the manuscript: 10.07.2021*